PCCP

# Probing spin effects in Phycocyanin using Janus-like ferromagnetic microparticles


| | |
|---|---|
| Journal: | *Physical Chemistry Chemical Physics* |
| Manuscript ID | CP-ART-10-2024-004129.R1 |
| Article Type: | Paper |
| Date Submitted by the Author: | 18-Dec-2024 |



| | |
|---|---|
| Complete List of Authors: | Schneider, Avi; Hebrew University of Jerusalem Department of Applied Physics<br>David, Ilay; Hebrew University of Jerusalem, Department of Applied physics<br>Goren, Naama; Hebrew University Department of Applied Physics<br>Fridman, Hanna; Hebrew University of Jerusalem, Department of Applied Physics<br>Lutzky, Guy; Technion Israel Institute of Technology, Schulich Faculty of Chemistry<br>Yochelis, Shira; 1Applied Physics Department and the Center for Nano-Science and Nano-Technology, The Hebrew University of Jerusalem, Jerusalem 91904 Israel, Applied Physics; Hebrew University,<br>Zer, Hagit; Hebrew University, Department of Applied Physics<br>Adir, Noam; Technion, Schulich Faculty of Chemistry<br>Keren, Nir; Hebrew University, Deptment of Plant & Environmental Science<br>Paltiel, Yossi; Hebrew University, Department of Applied Physics |
| | |

ARTICLE

# Probing spin effects in Phycocyanin using Janus-like ferromagnetic microparticles

Received 00th January 20xx,
Accepted 00th January 20xx

DOI: 10.1039/x0xx00000x

Avi Schneider[a], Ilay David[a], Naama Goren[a], Hanna T. Fridman[a], Guy Lutzky[b], Shira Yochelis[a], Hagit Zer[c], Noam Adir[b], Nir Keren[c] and Yossi Paltiel*[a]

In an era of interdisciplinary scientific research, new methodologies are necessary to simultaneously advance several fields of study. One such case involves the measurement of electron spin effects on biological systems. While magnetic effects are well known in biology, recent years have shown a surge in published evidence isolating the dependence on spin, rather than magnetic field, in biological contexts. Herein we present a simple method for the distinction between the two effects in solution-based samples. The induction of a single uniform spin upon molecules can be achieved by interacting them with a magnetized surface, thereby exposing them to controlled electron spin orientations. With many live biological systems, adsorption to a single surface severely limits the experimental output. Low signal to noise ratio from monolayers interacting with a relatively small surface area, and conformational restrictions due to immobilization, are common challenges when performing biological measurements on macroscopic magnetized surfaces. Here we demonstrate the use of Janus-like ferromagnetic microparticles, originally developed for a spin-based enantiomer separation procedure, as a platform for the spin-controlled measurement of biological molecules in solution. We find new evidence for electron spin involvement in biological systems, with influence observed on the kinetics, and to a lesser degree on the spectrum, of phycocyanin fluorescence. Our results provide both new scientific findings and proof of concept for the use of these unique magnetic particles as a flexible, soluble, high surface area, spin-controlled tool for scientific research.

## Introduction

Since the discovery of a unique relationship between chiral structures and the electron spin, termed the Chiral Induced Spin Selectivity (CISS) effect[1–3], there has been a growing interest in methodologies and model systems in which this phenomenon could be observed, studied, and utilized[4]. Simply put, the principle of CISS states that electrons passing through chiral molecules, or any charge displacements within a chiral molecule, are dependent on a correlation between the spin of the electrons and the molecule's enantiomeric form[5]. This interplay of electron spin and chiral molecules has been investigated and implemented in a wide range of fields, including spintronics[6], superconductivity[7], photovoltaics[8], chemical synthesis[9], and molecular biology[10] to name but a few[11]. Specifically, it was found that the chirality of a molecule affects its interaction with magnetic substrates[12]. Moreover, this interaction can be measured directly[13], and may be a key factor in protein folding[14] or enzymatic recognition[15]. In most previous examples, the prevalent technique for controlling the spin orientation of electrons participating in an experiment has been with magnetic surfaces in which electron spins can be uniformly aligned[16]. Though this approach has yielded much success in research and has been the basis for various applications[12,17–19], it is restricted by surface area considerations.

The need for direct interaction between target molecules and surfaces limits the influence on solution-born molecules using macroscopic magnetic substrates. This dictates certain constraints on the application or experiment and studied molecules or reactions must be sufficiently detectable as monolayers on the given surface area. Applications such as enantiomer purification on magnetized surfaces, for example, require multicycle processes and complex retrieval methods to mimic a large surface area[20,21]. To overcome these constraints, several studies have explored the use of magnetic particles to increase the available spin-controlled surface area and influence the molecules of interest in solution[14,22].

Although magnetic particles have been implemented in research, their practical benefits usually come at the expense of precision in control of spin orientation. The problem lies in the fact that any effectively magnetized particle will present one spin orientation on one of its sides and the opposite spin orientation on its other side, with both sides exposed to the

[a] Department of Applied Physics, Hebrew University, Jerusalem, Israel.
[b] Schulich Faculty of Chemistry, Technion, Haifa, Israel.
[c] Department of Plant & Environmental Sciences, The Alexander Silberman Institute of Life Sciences, Hebrew University of Jerusalem, Jerusalem, Israel.

* Corresponding author: Yossi Paltiel, Department of Applied Physics, Hebrew University of Jerusalem, Jerusalem 91904, Israel
Email: paltiel@mail.huji.ac.il

Supplementary Information available: [details of any supplementary information available should be included here]. See DOI: 10.1039/x0xx00000x

molecules in the solution. This means that the average interaction between molecules and particles is spin symmetric. For research questions in which a comparison between the influence of opposite spin orientations is needed, the symmetry must be broken. This is achieved at the expense of surface area in the standard use of magnetized surfaces which, being macroscopic and stationary, expose only one spin orientation to the solution. Furthermore, as magnetic effects have been observed and researched in biological systems[23,24], it is crucial to be able to differentiate between spin-induced and magnetically induced effects.

Braking of symmetry in particles has been achieved by *Metzger et al. (2020)* in the design of half covered ferromagnetic microparticles[25,26]. These particles, named Janus-like magnetic microparticles due to their non-intrinsic hetero-bi-faciality, present an exposed ferromagnetic surface on only one hemisphere. Though various materials, such as metals, metal-oxides and ionic crystals, display magnetic activity, their precise properties are often dictated by their dimensionality and crystal structure[27–30]. Thin films of pure, alloyed or doped transition metals are commonly used as planar ferromagnetic substrates, while Interesting properties have also been shown in low-dimensional materials such as monolayers and nanocrystals[31–33]. The magnetic behavior of the microparticles used in this study is derived from the shell of chromium oxide ($Cr_2O_3$) nanorods coated around their polystyrene core. While the chromium oxide surface of the particles possesses standard ferromagnetic properties, rather than the tunable magnetic characteristics displayed by some other materials[34,35], its partial exposure allows for the presentation of a single surface spin orientation. Once magnetized in a chosen orientation using an external magnetic field, the particles can be suspended in solution to interact with the molecules of interest. While these Janus-like ferromagnetic particles were originally implemented in enantiomer purification systems, here we demonstrate their use and potential for biological research. The particles were utilized here as a solution-based platform for the measurement of biomolecules under varying spin-controlled conditions. By interacting biomolecules with the pre-magnetized particles, it is possible to assess the influence of the induced spin conditions on the molecules in solution and compare between opposite spin interactions. This is done in the absence of an external magnetic field and can therefore, due to the very weak magnetic field induced by the particles themselves, narrow the variable experimental conditions to purely spin related ones.

The biomolecular signal studied here is the fluorescence of Phycocyanin, a photosynthetic chromophore-protein complex produced by cyanobacteria[36]. Phycocyanin is a member of the phycobiliprotein family, with a prosthetic tetrapyrrole molecule termed phycocyanobilin covalently bound to the amino acid backbone and serving as its chromophore[37,38]. The α-helix rich protein assembles into increasingly ordered structures. From a basic two-subunit monomer, trimeric and then hexametric rings are formed. They eventually assemble into rod like stacks of rings which further aggregate together with other phycobiliproteins into ordered clusters called phycobilisomes[36,37]. Phycocyanin absorbs light in the orange range of the visible spectrum, at wavelengths between 600 to 630 nm, and has a peak fluorescence at 642 nm[39]. In this work we investigate the influence of Janus-like particle magnetization on spectral and temporal aspects of phycocyanin fluorescence. Fluorescence spectrum measurements offer a steady state evaluation of the studied molecule under the conditions of its experimental environment. Fluorescence lifetime measurements are used frequently to characterize fluorescent emitters such as pigments, dyes, quantum dots and other photoactive molecules[40,41]. Unlike steady state measurements, fluorescence lifetime serves as a probe of dynamic processes and is indicative of the energy transfer pathways occurring in the emitter.

The anticipated chemical interactions between molecules and particles are mostly non-covalent electrostatic interactions between exposed functional groups of the protein and the metal oxide surface[42,43]. In addition to these, spin van der Wals and exchange interactions are also expected to occur[44,45]. Though the proteins are expected to interact strongly with the surface of the particles, this is likely to occur as a dynamic equilibrium rather than a permanent steady state, with a constant adsorption and desorption rate. This serves to maintain the asymmetry of the spin exchange interaction with the molecules, which is thought to only have a transient effect, not a permanent one, within the molecule[46,47]. Both the bare and ligand-covered sides of the particle are expected to interact with the protein, presenting chromium oxide and carboxylic groups, respectively. However, the long non-chiral ligands act as a barrier, preventing influence from spins of the coated surface, oriented antiparallelly to those on the exposed surface, creating an asymmetric effect.

Our results simultaneously show the existence of spin dependent behavior in Phycocyanin fluorescence, and the successful application of Janus-like ferromagnetic microparticles as a practical scientific research tool for spin-controlled measurement of biological samples in solution.

## Experimental

As aforementioned, this study consists of optical measurements, performed on Phycocyanin under varying surface spin conditions. It is important to stress that all measurements are made comparing between identical particles, with identical ligands, differing only by their magnetization properties. We rely on changes in optical parameters to infer changes in the structure or activity of these biomolecular systems. Changes in the fluorescence spectrum, for example, could point to different organizations of the biomolecule on the substrate. Changes in emission lifetime, on the other hand, are likely more specifically related to exciton dynamics. In all experiments, different spin conditions are induced through control of the electron spin orientation on the exposed surfaces of the Janus-like particles interacting with the molecules in solution.

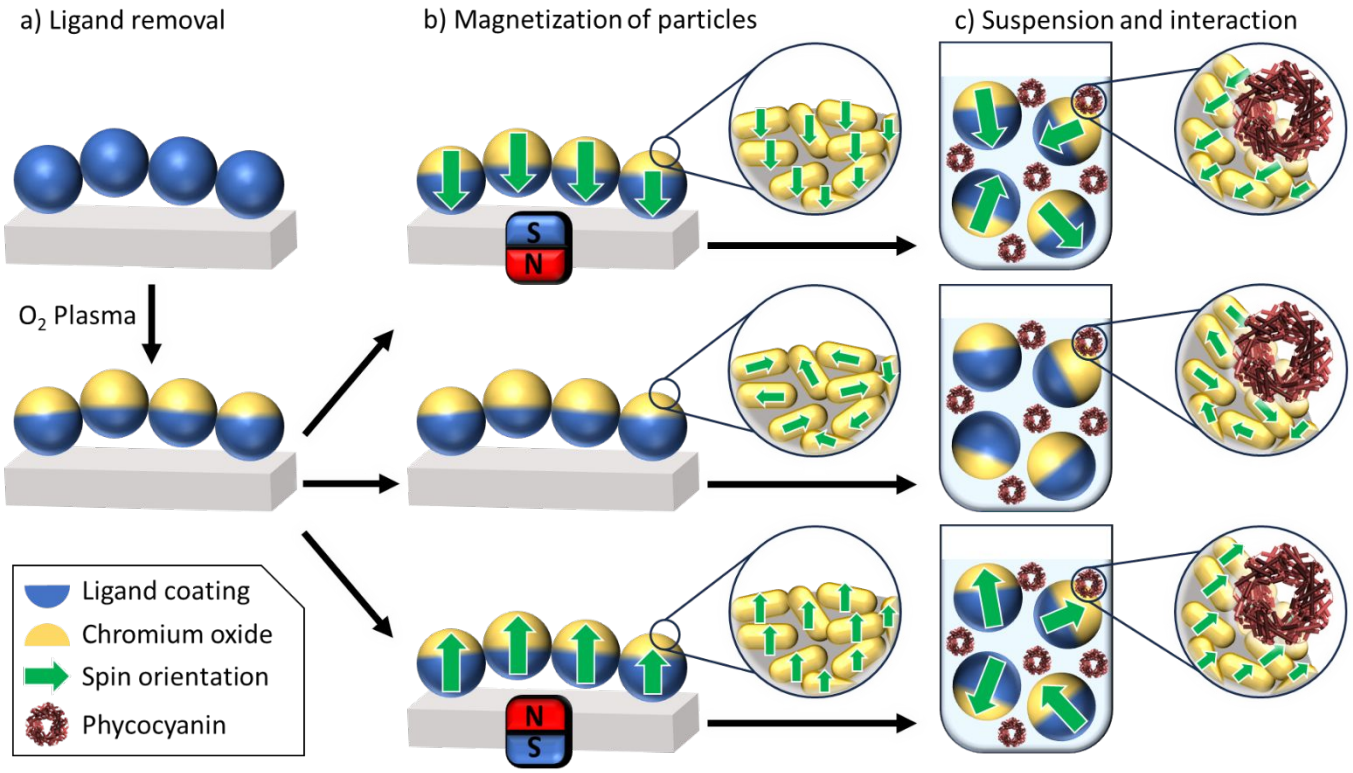


***Figure 1*** *– Preparation and Utilization of Janus-like ferromagnetic microparticle. The Janus particles are prepared in three stages. (**a**) The ferromagnetic microparticles are ordered on the substrate and the ligands are removed from the top of the particles with $O_2$ plasma. (**b**) The particles are either magnetized in a North or South orientation or are left at random magnetization. (**c**) The particles are removed from the substrate and suspended in the solution to interact with phycocyanin.*

The Janus-like microparticles used here were prepared, as first described in *Metzger et al. (2020)* and presented in Figure 1, by removing the organic ligand molecules from one hemisphere of the 4.7 µm diameter particles[26]. The Long hydrocarbon carboxylic acid ligands were removed from the top surface of immobilized particles using oxygen plasma, thereby exposing the chromium oxide on only one side of the particles. While still in film form, the half-exposed particles were uniformly magnetized perpendicularly to their surface. In this magnetization process, surface electron spins are aligned in either an up or down orientation by applying an external magnetic field using a 0.5T permanent magnet. This produces chemically identical particles differing only by the opposite magnetization of their exposed surface. The ferromagnetic nature of the chromium oxide nanorods (Figure 2a) allows for the chosen spin orientation to be maintained steadily once the external field is removed. For control samples, no external magnetic field was applied, and the spin orientation in the chromium oxide nanorods remained random and non-uniform, yielding on average no net magnetization of the exposed part of the microparticles. Once the spin conditions were induced, the microparticles were resuspended and introduced in solution to Phycocyanin hexamers (Figure 2b). The pre-magnetized Janus-like particles were designed to expose either a north or south magnetic pole to the solution, presenting either up or down oriented surface electron spins to the interacting proteins, respectively. Non-magnetized particles, presenting a random surface spin orientation, were also tested, as well as pure phycocyanin proteins without the Janus-like particles.

Fluorescence emission spectra of phycocyanin were measured as probes of the pigment's steady state configuration and its links to the environment[48]. The spectra were measured between 620 and 700 nm, using an excitation wavelength of 590 nm. Four types of spin conditions were tested, with protein samples containing either north, south or non-magnetized microparticles as well as a control sample containing only proteins and no particles.

To investigate spin related dynamics, fluorescence lifetime measurements of Phycocyanin were conducted under the different spin conditions induced by the particles. Fluorescence decay curves and lifetimes were obtained using a Time Correlated Single Photon Counting (TCSPC) measurement in which the sample is repeatedly excited using a monochromatic pulsed laser and the relative time of emission is recorded [14,49]. Excitation was induced at a wavelength of 600nm, and the emitted photons were collected in the range of 630-650nm with a temporal resolution of 40 picoseconds. This method yields a histogram of emission times which is correlative to a fluorescence decay curve. Once collected, the histograms are fitted with an exponential decay function. Lifetime values are

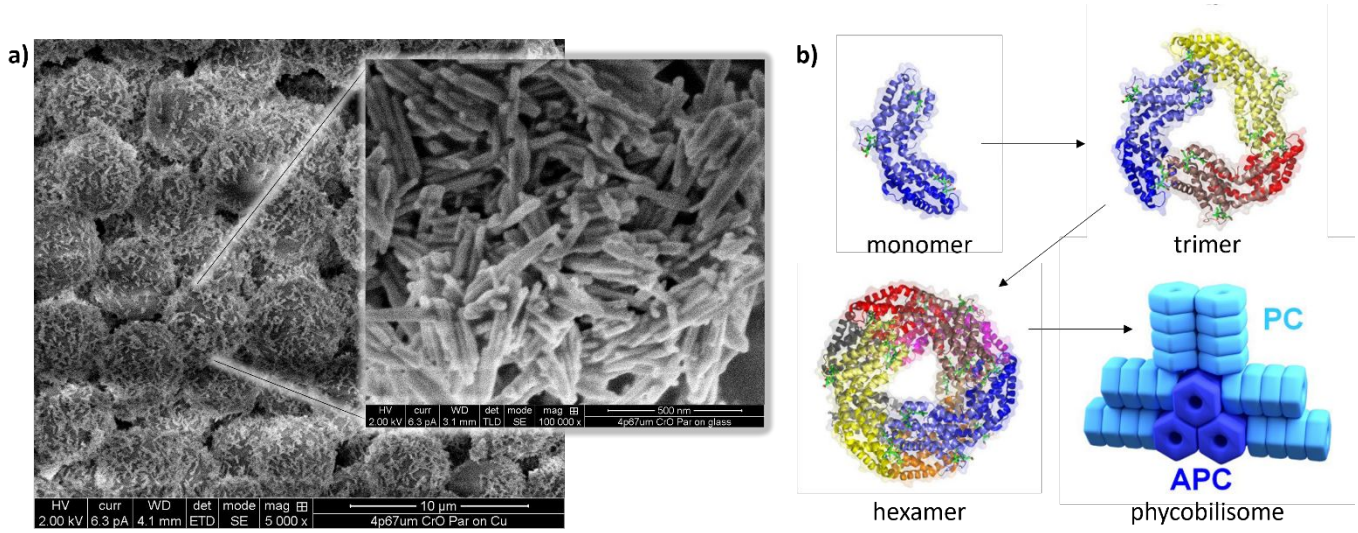


***Figure 2** – (**a**) SEM image of Janus particles showing chromium oxide nanorods on surface. (**b**) model of phycocyanin molecule and assemblies (taken with permission from Photosynthesis Research[48])*

then calculated as the time, from excitation, at which the fitted exponent function has decayed to 1/*e* of the initial maximal fluorescence value[50]. The decay curves and lifetime values were measured and compared for phycocyanin interacting in solution with either up, down, or non-magnetized Janus-like ferromagnetic microparticles, as well as in its pure form. To probe higher moments of the signal, noise analysis of the signal fluctuation intensity was performed on the time resolved fluorescence curves, producing a deviation histogram for each measured condition[51]. This analysis supplies richer information on the differences in dynamics between the magnetic conditions of the particles as compared to the decaying lifetime signal only.

## Results

### Fluorescence emission

The fluorescence emission spectra of phycocyanin are shown in Figure 3 for molecules interacting with differently magnetized Janus-like particles. The emission spectra present a broadening induced by all particles, with a more pronounced long-wavelength shoulder observed in the case of north magnetization compared with the other two conditions. The emission peak is observed at approximately 640 nm for all conditions. As a change in the Phycocyanin structure upon adsorption to surface is expected to affect its spectrum, the broadening of emission spectra, in the presence of all particles, is likely indicative of direct interaction between the measured phycocyanin and the particles. The excitation spectral response, presented in the SI Figure S5, supplies additional indication of protein interaction with the particles. The near identical emission maxima and relatively similar spectra, obtained for all magnetization conditions, suggest no major changes induced to phycocyanin by each surface spin condition uniquely. However, while various conditions, such as pH, aggregation, solvent or crowding, may cause spectrum broadening and shoulders[48], these conditions were maintained as similar as possible in all measured samples. Therefore, the distinct shoulder feature observed on the long-wavelength slope of the spectrum, specifically with north-magnetized particles and not with the otherwise identical south- and non-magnetized particles, suggests the involvement of a spin induced effect.

### Fluorescence lifetime

When examining the time-resolved fluorescence curves under the different conditions (Figure 4a), similarly to the spectral measurements it can be observed that interaction with all

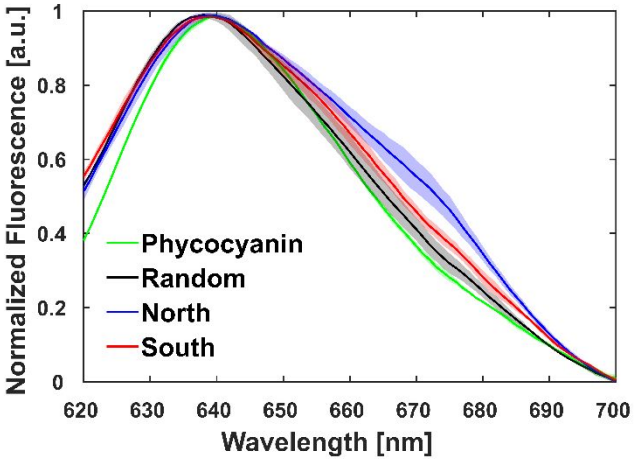


*phycocyanin without (green) and with north (blue), south (red), or randomly (black) magnetized Janus-like particles. The spectra are normalized and averaged (n=4) with the shaded areas representing the standard deviation between measurements. The spectra were obtained using a 590 nm excitation wavelength and measuring the emission in the wavelength range of 620 to 700 nm.*

particle types induces a faster fluorescence decay compared to that of pure phycocyanin. This too may be indicative of a general effect induced by the mere adsorption of the phycocyanin molecules to the particle surface, regardless of surface spin. However, for phycocyanin in the presence of the different surface-spin-oriented particles, a distinct difference can be observed between the decay with non-magnetized particles and those with either up or down magnetized particles (Random, North or South, respectively). The decay of fluorescence clearly appears to be slower in the case of uniformly oriented surface spins, regardless of direction, compared to randomly oriented spins. When analyzing the behavior of the fluorescence decay through curve fitting (SI Figure S7), pure phycocyanin and both north and south magnetization results were found to be sufficiently described by a mono-exponential decay function, while random magnetization curves were better fitted using a bi-exponential decay function. This can also be seen in the Goodness of Fit (GOF) indexes of the different conditions, where both standard and Poisson-corrected reduced $X^2$ values support the same conclusions. Figure 4b shows the calculated lifetimes under the different magnetizations. The lifetimes of north and south magnetizations (1.24ns and 1.26ns respectively) reflect prolonged fluorescence under these uniform conditions, compared with the first term lifetime of the random magnetization (0.84ns). As mentioned, pure phycocyanin displays the longest lifetime (1.36ns). The second term lifetime of random magnetization is longer (1.69ns) but contributes less to the overall decay, as represented by its term amplitude (~55% of the first term). This is, however, a non-negligible second term amplitude when compared to those calculated for north and south magnetizations, as well as pure phycocyanin, using a bi-exponential fit (~13%, ~7% and ~3% of the first term, respectively), reflecting the near mono-exponential behavior of these decays. Fit quality indexes and calculated coefficients, using both mono- and bi-exponential fits, as well as different data time windows, are compared and presented in the Supplementary Information Figures S7, S8 and S9. Average values and standard errors of all calculated fit parameters and GOF indexes are summarized in SI tables S1, S2 and S3, including the various formulas used. In addition to the prominent difference between uniform and random magnetizations, a much smaller shift appears to be correlated to the orientation of magnetization, with a minor delay in the fluorescence decay for south magnetization compared with north magnetization.

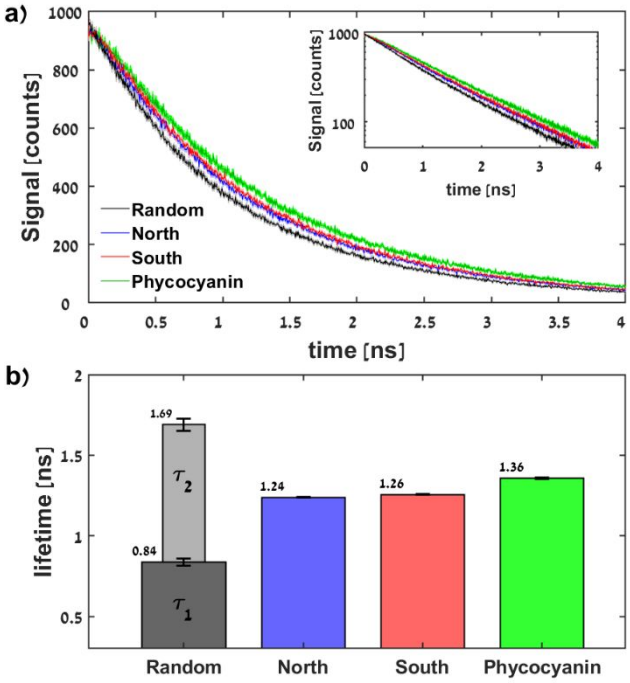


***Figure 4*** *- Time resolved fluorescence measurements of Phycocyanin under different spin conditions induced by the Janus-like particles. (**a**) Fluorescence decay curves measured for phycocyanin alone (green) and with north (blue), south (red) or randomly (black) magnetized particles. The dark lines represent the measured data averaged over 8 samples, and the lighter shaded areas represent the standard error. The inset is a semi-logarithmic presentation of the same. (**b**) Average lifetimes calculated from the fits, with one decay coefficient for the mono-exponential-like pure phycocyanin and uniform magnetizations, and two for the bi-exponential-like random magnetization. For random magnetization the first term lifetime is represented by the dark bar and the second term lifetime by the faded bar, with the width ratio of the bars corresponding to the amplitude ratio of both terms in the bi-exponential decay.*

**Noise analysis**

Noise analysis of the fluorescence decay measurements supplies additional information through the distribution of signal fluctuations around the fluorescence decay curve (Figure 5). These histograms reveal different noise distribution patterns for the four experimental conditions. Randomly produced fluctuations in the intensity of biological signals are expected to display a gaussian distribution around the central signal value. Here, multiple gaussian fitting of the noise distribution histograms (SI Figure S10) shows that, in addition to a wide-band low-amplitude gaussian present in all cases, the four distributions appear to be comprised of a differing ensemble of gaussian curves. While the north and south magnetized particles display two prominent gaussian distributions, the randomly magnetized particles and pure phycocyanin present three prominent gaussian distributions. Each with one gaussian smaller than the other, the north and south conditions display a somewhat opposite arrangement of their two peaks. The three gaussians of pure phycocyanin and random conditions show similar size ratios, however they differ in order and position. Additional analysis of noise pattern dependence on fit type and time window is presented in SI Figures S11, S12, S13 and S14, suggesting a time basis for the different appearing features. While definitive understanding of the involved mechanisms cannot be directly derived from these analyses and

proposed fits, their features consistently reveal underlaying differences which hint at distinct non-random factors influencing the fluctuations. Displaying dependency on particle magnetization, Such factors are likely to be electron spin related, and may be linked to charge separation and the generation of singlet or triplet excitons in the chiral structures [52,53].

## Discussion

An isolated phycocyanin unit can be considered as a set of two-level systems in which light energy drives the population of the excited states with de-excitation occurring through fluorescence or heat[48,54]. Protein structures are chiral on multiple levels, from the amino acid building blocks to the alpha-helix-rich secondary structure and the multi-subunit organization of the quaternary structure. These chiral structures and domains are expected, according to the CISS affect, to generate inhomogeneous electron spin distributions as a consequence of charge polarization or charge redistribution[5]. This means that a chiral protein environment induces spin accumulation and therefore affects the electronic properties of the protein, and its interaction with magnetic or spin controlled surfaces. In such chiral systems, under varying spin conditions, the fluorescence dynamics are likely to be affected, as was observed here.

The steady-state spectral properties of the phycocyanin show a broadened spectrum for particle-associated pigments, with the fluorescence maximum is itself not affected, implying that the emitting states are similar. The red shifted shoulder in the case of north magnetization, however, could be indicative of a spin dependence, such as higher adsorption affinity of the protein to the uniformly up oriented surface spins of the particle. A more conclusive spin dependence is observed in TCSPC measurements, where the decay behavior and signal fluctuations are influenced differently by the presence of the differently magnetized particles.

While the fluorescence lifetime is decreased in the presence of all particle types, compared to pure phycocyanin, a clear difference can be observed in both the nature and rate of fluorescence decay when measured with randomly and uniformly magnetized particles. The bi-exponential nature of the fluorescence decay in the presence of randomly magnetized particles, compared to the mono-exponential one seen with uniform magnetization, warrants speculation as to possible mechanisms behind this difference. Additionally, the longer fluorescence lifetimes measured with uniform magnetization imply longer-lived charge separation in the excited system, suggesting different energy pathways induced by each condition. These differences might be attributed to scenarios of zero versus non-zero spin states, correlating to random or

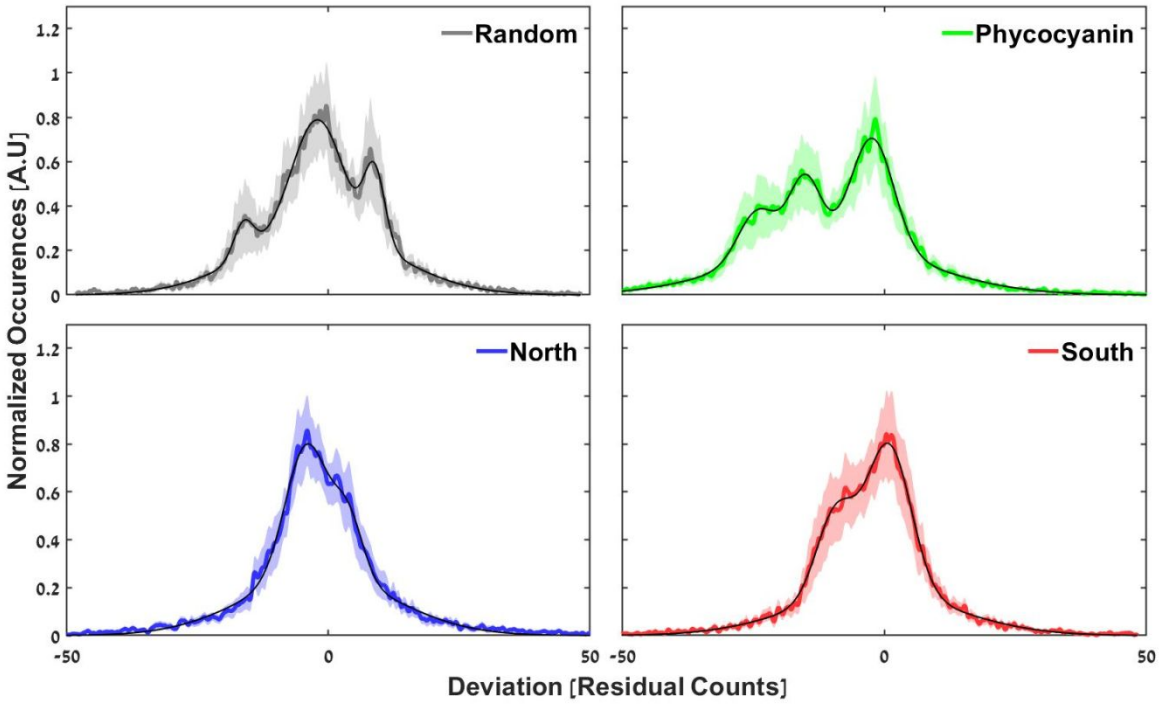


***Figure 5 -*** *Noise fluctuation histograms calculated from the measured decay curves under the four different experimental conditions. The distributions plot the relative occurrence of fluctuations as a function of their deviation from the calculated bi-exponential fit of the measured fluorescence decay curves. The dark, bold colored lines represent averaged (n=8) histograms for each particle magnetization and for pure phycocyanin, while the light shaded colored areas represent the standard error within the analyzed individual histograms. The thin black lines are the proposed fits to the distributions, obtained using multiple gaussian distributions.*

uniform spin alignments, respectively. Non-zero spin pathways, such as the formation of triplet excitons through direct asymmetric excitation or intersystem crossing, might be facilitated by uniform surface spin conditions in the interacting particle. Radiative processes in such triplet states are restricted by a forbidden relaxation to the singlet ground state and are therefore associated with longer lifetimes[41,50,55]. The non-zero spin conditions, expected within the chiral environment of the protein, could possibly further support triplet exciton formation and stability over the zero-spin singlet state, potentially increasing triplet population, prolonging charge separation and extending fluorescence lifetimes[56]. This might also account for the mono-exponential behavior of the fluorescence decay in pure phycocyanin, which is not externally spin-influenced but possesses intrinsic spin conditions through its chirality. In the case of random surface spin alignment, which shows both a faster fluorescence decay and a bi-exponential behavior we might speculate that both singlet and triplet excitons are naturally generated. The relaxation pathways of both populations contribute to the overall fluorescence decay, with the more abundant singlet excitons represented by the short-lifetime large-amplitude first term and the triplet excitons by the second term of the bi-exponential fit.

Interestingly, while we observe a difference between the fluorescence spectra obtained with north and south magnetizations, their fluorescence decay curves show no substantial differences. This might be the result of differences in the coupling between the electron spins in the particle (dictated by magnetization) and those in the protein (dictated by chirality). The effect might be manifested as stabilization or destabilization of the local spin distribution in the protein and therefore might dictate a preferred adsorption orientation of the protein on the particle.

The different coupling influenced the energy of some of the emitting states, as seen in the spectral shoulder, but not the exciton longevity, as seen by the similar lifetimes. It is possible that certain structural and chemical changes in the environment of the emitting chromophore were induced by the interaction with north magnetized particles, but not by the south or randomly magnetized ones. While these changes might affect the energy of the emitting state, and therefore the wavelength of fluorescence, they do not necessarily also impact the type of exciton formed and its path and stability within the protein. The opposite statements might also be made, where significant differences in fluorescence lifetime, as between south and random magnetizations, do not translate into fluorescence spectrum differences.

The observed differences are further substantiated by the noise analysis, where we find distinctly unique patterns of signal fluctuations for all four experimental conditions. From this analysis we recognize that pure phycocyanin and randomly magnetized particles produce a noise pattern with three clear peaks, and that south and north magnetized particles show two peaks. The different patterns possibly indicate changes in the accessibility of competing energy pathways in a multi-level quantum system[52]. While both zero-spin cases of random magnetized particles and no particles (pure phycocyanin) show a complex noise pattern comprised of at least three peaks, their occurrence and deviation distributions are different. Whereas with random magnetization the peak cluster seems relatively symmetrically dispersed around the central signal, the pattern with pure phycocyanin is asymmetrically shifted towards weak signal fluctuations.

The non-zero spin cases of north and south magnetizations show a less complex noise pattern, but also display a certain directionality which is opposite regarding each other. These patterns might correspond to the same trend observed in the decay curves themselves, with the intrinsic spin asymmetry of the chiral protein being either enhanced or diminished by the externally induced uniform or random spin conditions, respectively. Additionally, the time-dependence of the different features in the noise distributions suggests a correlation to the longevity of the excited states. which, due to differences in their symmetry, is also likely to be influenced by the chiral potential of the protein.

An additional mechanism which should be considered is that of charge transfer between the protein and particles, as it might be involved in the general shortening of fluorescence lifetime observed with all particle types. This charge transfer between the excited protein and the particles could also be influenced by the uniformity of their surface spins. This would constitute an alternative non-radiative mechanism by which phycocyanin fluorescence lifetime might be influenced differently by particle magnetization in a zero or non-zero spin scenario. While the precise mechanism cannot be determined by these results alone, we believe that additional methods, such as transient absorption spectroscopy, could be used to investigate this hypothesis.

While observations of electron spin involvement in different biosystems have been documented before, using magnetic surfaces[10,14,57], this work presents additional evidence of this phenomenon and introduces new experimental methodologies by which it can be investigated. It demonstrates a successful implementation of Janus-like ferromagnetic particles and shows their potential as a powerful research tool without the need of a single large surface. The induction of different surface spin conditions on otherwise identical particles offers the possibility of examining spin effects on biological systems in solution, while overcoming surface area limitations encountered in previous studies[14]. The implications of such spin effects span from questions regarding the origin of homochirality in biology, through better understanding of intra and inter peptide interactions, to possible medical application of spin-controlled platforms to manipulate biological function.

## Summary

While magnetic field effects in biology are well established, the recent understanding of direct electron spin involvement in biological processes necessitates the ability to differentiate

between the two effects. We present a novel experimental platform, based on chemically identical particles, and no external magnetic field, for the direct probing of spin related effects in biological systems, in solution. The fluorescence properties of phycocyanin molecules were investigated under various electron spin conditions, induced using Janus-like magnetic microparticles. Both spectral and time resolved measurements were conducted on phycocyanin in either its pure form or interacting with north-, south- or non-magnetized particles, presenting up, down or randomly oriented surface spins, respectively. While a small effect was observed in the fluorescence spectrum of phycocyanin in response to the different induced spin conditions, lifetime measurements revealed a clear temporal effect. Uniform spin orientation of the particle surface induced prolonged fluorescence lifetimes and a mono-exponential decay, compared to shorter lifetimes and a bi-exponential decay seen with random spin orientation. Further analysis of fluorescence signal noise fluctuations suggests that the introduction of a uniform spin reduces the energy landscape complexity. While consolidating the difference between the random and uniform spin conditions, the noise analysis also suggests that the north and south magnetizations induce slightly different relaxation mechanisms. This difference might be caused by the coupling of the induced spins to the predetermined chiral environment of the protein and is perhaps responsible for the minor differences in fluorescence lifetimes and spectra observed between these conditions. We offer two, non-mutually exclusive hypotheses, of triplet formation through intersystem crossing and charge transfer with particles, as possible mechanisms for these effects. These results suggest that electron spin plays a critical role in the function of the phycocyanin light harvesting protein, possibly due to influences induced by the chiral protein environment. Our findings shed new light on the relationship between electron spin and biological processes and demonstrate the novel use of Janus-like magnetic microparticles as a spin controlled experimental method for biomolecules.

## Methods and materials

### *Janus-like microparticle preparation*

The Ferromagnetic Janus-like microparticles were prepared as described in *Metzger et al. MethodsX 2020* using chromium oxide coated polystyrene microparticles of 4.7 μm diameter (*Spherotech – Carboxyl Ferro-Magnetic Particles – CFM-40-10)*. 100 μl droplets of the particles, at a concentration of 0.25% w/v, were dried on glass slides at 60℃ and the carboxylic acid ligands were removed from the exposed hemisphere of the particles using 100% oxygen plasma for 10 minutes at 50% power in a Plasma Asher (*Diener electronic*). The particles were then magnetized while still immobilized and aligned (ligand-free hemisphere up) on the slides using a permanent 0.5 tesla magnet. They were then removed from the slides using a 50mM Tris HCl (pH 7.5) buffer and a pipette tip for scraping. The particles were then resuspended in the buffer at a concentration of 0.25% w/v to be added to the protein solutions. The stability of particle magnetization was validated through contact angle measurements, presented in SI Figures S1, S2 and S3.

### *Phycocyanin expression and purification*

The phycocyanin proteins were harvested from cultured *Thermosynechococcus vulcanus* (*T. Vulcanus*) cyanobacteria. *T. vulcanus* culture was grown in a 10L stirred growth tank and kept at 55℃ using a hotplate. A constant flow of $CO_2$-enriched air (5%) was bubbled into the culture at a gas flow rate of 1 L/min per liter of sample, and the pressure was vented through a specialized cap. The media used was BG11, appropriate for growth of freshwater cyanobacteria cultures. The cultures were exposed to constant white LED lighting. After 7-30 days of growth, the culture was centrifuged using a swing rotor at 5000xg, creating a solid pellet. The pellets were combined, weighed, and resuspended in 30mL of Isolation Buffer A before being stored at -20℃.

The resuspended frozen samples were thawed to room temperature, sifted through gauze, and homogenized using a hand-held homogenizer. The lysis process was done using Constant Systems' Cell Disrupter model TS2 CF1 high-pressure cell disruption device. The cells were lysed using 40,000 KPSI, and the temperature was kept at 4℃ using the attached cooling jacket. To separate whole cells, membrane fragments, and other insolubilized materials, the lysate was centrifuged at 14,500 RPM for 30 minutes at 4℃ using a fixed rotor. The resulting pellet was then characterized using a Nanodrop spectrophotometer to validate that it does not contain our target protein. The supernatant fraction was then incubated for 1 hour in a 20% v/v solution of saturated ammonium sulfate at 4℃. The resulting solution was centrifuged at 14,500 RPM for 30 minutes using a fixed rotor to separate the precipitated proteins from our target protein. This procedure was repeated using 50% v/v saturated ammonium sulfate solution, precipitating the phycobiliproteins from the solution. A dialysis step was performed overnight at 4℃ using a 100-fold volume of Isolation Buffer A and a 20mL Mega GeBaflex dialysis kit. Chromatographic separation was used to isolate our target proteins from other proteins that may still be in our sample solution and separate different phycobiliproteins from one another in different fractions. The chromatography was done using a 35mL column manually packed with Q Sepharose Fast Flow Resin, and a gradient of Isolation Buffer A and Isolation Buffer B. The fraction containing phycocyanin was retrieved and used in the described experiments.

### *Phycocyanin fluorescence measurements with Janus-like ferromagnetic particles*

Phycocyanin solutions of 3g/L in 50mM Tris HCl (pH 7.5) were prepared by 1:100 dilution of a 300g/L protein stock solution. The solutions were introduced to the prepared Janus-like particles at a volume ratio of 1:10. The particles were then precipitated and resuspended in clean medium to remove excess free-floating proteins. The process was repeated for the different particle magnetizations, yielding three distinct protein-particle solutions representing up, down and random surface spin conditions. Interaction measurements were conducted using fluorescence decay curves obtained with the supernatant and precipitate of protein-particle suspensions (Figure S15).

The fluorescence excitation and emission spectra of the phycocyanin under varying conditions were obtained using a *Horiba* fluorometer into which 2 ml of each sample were placed in quarts four sided cuvettes. Samples containing Janus-like particles, but no protein were used as a blank. Emission spectra were measured between 620 and 700 nm using an excitation wavelength of 590 nm. Excitation spectra were obtained by measuring emission at 640 nm while scanning excitation between 560 and 630 nm. The absorbance and scattering of the Janus-like particles in the range of the phycocyanin absorption peak makes measurements in that part of the spectrum difficult and yields a low signal to noise ration ratio. Both excitation and emission slits were set to 8 nm bandwidth, and a neutral density (ND 0.5) filter was used for the measurement of pure phycocyanin.

Fluorescence decay measurements of the different protein-particle samples, and pure phycocyanin, were performed using a time-correlated single-photon counting (TCSPC) technique. 2 ml samples were placed in a quartz cuvette and time-resolved photoluminescence measurements were conducted. Phycocyanin excitation was induced using a *Fianium WhiteLase SC-400* supercontinuum pulsed laser, at a repetition rate of 10MHZ, monochromatized to the peak phycocyanin absorption at 600nm. Emitted light was collected and filtered using a 640nm band-pass filter with a 20nm bandwidth. The measurement setup is illustrated in the Supplementary Information (Figure S6). A *Picoharp* Time to Amplitude converter (TAC) and its accompanying software were used to synchronize between excitation pulse and emitted photon detection to produce histograms of photon count as a function of time. Due to limited signal intensity caused by light scattering off Janus-like particles, acquisition was set to terminate when reaching a relatively low maximum of 1000 counts, to maintain reasonable measurement lengths. The obtained histograms were analysed to determine the average fluorescence lifetimes through tail fitting to both mono- and bi-exponential decay functions. Various time windows of the measured data (8, 6, and 4 nanoseconds) were used for the fitting and are compared, along with single and double exponents, in SI Figures S7, S8, and S9, and are summarized in SI tables S1, S2 and S3.

Fluorescence noise histograms were produced using custom written MATLAB scripts. They were fitted with multiple gaussian distributions (Figure S10) and their normality was assessed using Q-Q plots (Figure S11), showing that the majority of the noise, centered around the measured signal, falls into a gaussian like distribution pattern. The noise histograms were evaluated using the various fit types and time windows, as presented in SI Figures S12, S13 and S14.

## Author contributions

Conceptualization by AS, HF, SY, NK and YP. Resources by GL, AS and ID. Investigation by AS and ID. Formal analysis by AS, ID and NG. Project Administration by HZ and SY. Supervision by NK and YP. Visualization and Writing (Original Draft) by AS. Writing (Review & Editing) by AS, SY, NA, NK and YP.

## Conflicts of interest

There are no conflicts to declare.

## Data availability

Data for this article, including [description of data types] are available at [name of repository] at [URL – format https://doi.org/DOI].

## Acknowledgements

We thank Ofek Vardi, Nadav Ben Eliezer and Yael Kapon, of the Hebrew University, for their assistance during experimental work and analysis. We Thank Lech Tomasz Baczewski, of the Polish academy of sciences, for the use of his ferromagnetic substrates in our experiments.

## References

1 K. Ray, S. P. Ananthavel, D. H. Waldeck and R. Naaman, *Asymmetric Scattering of Polarized Electrons by Organized Organic Films of Chiral Molecules*, 1999, vol. 283.

2 B. Göhler, V. Hamelbeck, T. Z. Markus, M. Kettner, G. F. Hanne, Z. Vager, R. Naaman and H. Zacharias, Spin selectivity in electron transmission through self-assembled monolayers of double-stranded DNA, *Science (80-. ).*, 2011, **331**, 894–897.

3 R. Naaman and D. H. Waldeck, Chiral-induced spin selectivity effect, *J. Phys. Chem. Lett.*, 2012, **3**, 2178–2187.

4 B. P. Bloom, Y. Paltiel, R. Naaman and D. H. Waldeck, Chiral Induced Spin Selectivity, , DOI:10.1021/acs.chemrev.3c00661.

5 R. Naaman, Y. Paltiel and D. H. Waldeck, *Annu. Rev. Biophys.*, 2022, 51, 99–114.

6 R. Naaman and D. H. Waldeck, *Annu. Rev. Phys. Chem.*, 2015, 66, 263–281.

7 H. Alpern, E. Katzir, S. Yochelis, N. Katz, Y. Paltiel and O.

Millo, Unconventional superconductivity induced in Nb films by adsorbed chiral molecules, *New J. Phys.*, , DOI:10.1088/1367-2630/18/11/113048.

8 J. Wang, H. Lu, X. Pan, J. Xu, H. Liu, X. Liu, D. R. Khanal, M. F. Toney, M. C. Beard and Z. V. Vardeny, Spin-Dependent Photovoltaic and Photogalvanic Responses of Optoelectronic Devices Based on Chiral Two-Dimensional Hybrid Organic-Inorganic Perovskites, *ACS Nano*, 2021, **15**, 588–595.

9 T. S. Metzger, S. Mishra, B. P. Bloom, N. Goren, A. Neubauer, G. Shmul, J. Wei, S. Yochelis, F. Tassinari, C. Fontanesi, D. H. Waldeck, Y. Paltiel and R. Naaman, The Electron Spin as a Chiral Reagent, *Angew. Chemie Int. Ed.*, 2020, **59**, 1653–1658.

10 K. Banerjee-Ghosh, S. Ghosh, H. Mazal, I. Riven, G. Haran and R. Naaman, Long-Range Charge Reorganization as an Allosteric Control Signal in Proteins, *J. Am. Chem. Soc.*, 2020, **142**, 20456–20462.

11 R. Naaman, Y. Paltiel and D. H. Waldeck, Chiral Molecules and the Spin Selectivity Effect, *J. Phys. Chem. Lett.*, 2020, **11**, 3660–3666.

12 K. Banerjee-Ghosh, O. Ben Dor, F. Tassinari, E. Capua, S. Yochelis, A. Capua, S. H. Yang, S. S. P. Parkin, S. Sarkar, L. Kronik, L. T. Baczewski, R. Naaman and Y. Paltiel, Separation of enantiomers by their enantiospecific interaction with achiral magnetic substrates, *Science (80-. ).*, 2018, **360**, 1331–1334.

13 Y. Kapon, A. Saha, T. Duanis-Assaf, T. Stuyver, A. Ziv, T. Metzger, S. Yochelis, S. Shaik, R. Naaman, M. Reches and Y. Paltiel, Evidence for new enantiospecific interaction force in chiral biomolecules, *Chem*, 2021, **7**, 2787–2799.

14 H. M. Levy, A. Schneider, S. Tiwari, H. Zer, S. Yochelis, P. Goloubinoff, N. Keren and Y. Paltiel, The effect of spin exchange interaction on protein structural stability, *Phys. Chem. Chem. Phys.*, 2022, **24**, 29176–29185.

15 Q. Zhu, Y. Kapon, A. M. Fleming, C. J. Burrows, Y. Paltiel and R. Naaman, The role of electrons' spin in DNA oxidative damage recognition, *Cell Reports Phys. Sci.*, 2022, **3**, 101157.

16 C. Rau, Electron spin polarization esp at surfaces of ferromagnetic metals, *J. Magn. Magn. Mater.*, 1982, **30**, 141–174.

17 H. Al-Bustami, S. Belsey, T. Metzger, D. Voignac, S. Yochelis, O. Shoseyov and Y. Paltiel, Spin-Induced Organization of Cellulose Nanocrystals, , DOI:10.1021/acs.biomac.2c00099.

18 T. S. Metzger, R. Siam, Y. Kolodny, N. Goren, N. Sukenik, S. Yochelis, R. Abu-Reziq, D. Avnir and Y. Paltiel, Dynamic Spin-Controlled Enantioselective Catalytic Chiral Reactions, *J. Phys. Chem. Lett. 2021*, 2024, **12**, 32.

19 N. Goren, ‖ Tapan, K. Das, N. Brown, S. Gilead, S. Yochelis, E. Gazit, R. Naaman and Y. Paltiel, Metal Organic Spin Transistor, 2024, **14**, 27.

20 F. Tassinari, J. Steidel, S. Paltiel, C. Fontanesi, M. Lahav, Y. Paltiel and R. Naaman, Enantioseparation by crystallization using magnetic substrates, *Chem. Sci.*, 2019, **10**, 5246–5250.

21 K. Santra, D. Bhowmick, Q. Zhu, T. Bendikov and R. Naaman, A Method for Separating Chiral Enantiomers by Enantiospecific Interaction with Ferromagnetic Substrates, *J. Phys. Chem. C*, 2021, **125**, 17530–17536.

22 A. Narayanan Nair, S. Fernandez, M. Marcos-Hernández, D. R. Romo, R. Singamaneni, D. Villagran and S. T. Sreenivasan, Spin-Selective Oxygen Evolution Reaction in Chiral Iron Oxide Nanoparticles: Synergistic Impact of Inherent Magnetic Moment and Chirality, , DOI:10.1021/acs.nanolett.3c02752.

23 M. F. Barnothy, Ed., *Biological Effects of Magnetic Fields*, Springer US, Boston, MA, 1964.

24 K. Schulten, in *Festkörperprobleme, Advances in Solid State Physics*, ed. P. G. Aachen, Springer Berlin Heidelberg, Berlin, Heidelberg, 1982, vol. 22, pp. 61–83.

25 T. S. Metzger, Y. Tokatly, E. Avigad, S. Yochelis and Y. Paltiel, Selective enantiomer purification using magnetic oriented interacting microparticles, *Sep. Purif. Technol.*, 2020, **239**, 116501.

26 T. S. Metzger, A. Schneider, N. Goren, A. Ziv, Y. Tocatly, E. Avigad, S. Yochelis and Y. Paltiel, Magnetic oriented microparticles preparation, *MethodsX*, 2020, **7**, 100975.

27 D. Vollath, D. V. Szabó and J. O. Willis, Magnetic properties of nanocrystalline Cr2O3 synthesized in a microwave plasma, *Mater. Lett.*, 1996, **29**, 271–279.

28 U. Balachandran, R. W. Siegel, Y. X. Liao and T. R. Askew, Synthesis, sintering, and magnetic properties of nanophase Cr2O3, *Nanostructured Mater.*, 1995, **5**, 505–512.

29 S. A. Makhlouf, Magnetic properties of Cr2O3 Nanoparticles, *J. Magn. Magn. Mater.*, 2004, **272–276**, 1530–1532.

30 M. Ba obre-L pez, C. V zquez-V zquez, J. Rivas and M. A. L pez-Quintela, Magnetic properties of chromium (III) oxide nanoparticles, *Nanotechnology*, 2003, **14**, 318–322.

31 W. Xun, C. Wu, H. Sun, W. Zhang, Y.-Z. Wu and P. Li, Coexisting Magnetism, Ferroelectric, and Ferrovalley Multiferroic in Stacking-Dependent Two-Dimensional Materials, *Nano Lett.*, 2024, **24**, 3541–3547.

32 P. Li, X. Li, J. Feng, J. Ni, Z.-X. Guo and H. Xiang, Origin of zigzag antiferromagnetic order in XPS3 (X = Fe, Ni) monolayers, *Phys. Rev. B*, 2024, **109**, 214418.

33 S. Yang, C. Feng, D. Spence, A. M. A A Al Hindawi, E. Latimer, A. M. Ellis, C. Binns, D. Peddis, S. S. Dhesi, L. Zhang, Y. Zhang, K. N. Trohidou, M. Vasilakaki, N. Ntallis, I. MacLaren and F. M. F de Groot, Robust Ferromagnetism of Chromium Nanoparticles Formed in Superfluid Helium, , DOI:10.1002/adma.201604277.

34 P. Li and Z.-X. Guo, The Dirac half-semimetal and quantum anomalous Hall effect in two-dimensional Janus $Mn_2X_3Y_3$ (X, Y = F, Cl, Br, I), *Phys. Chem. Chem. Phys.*, 2021, **23**, 19673–19679.

35 P. Li, X. Yang, Q. S. Jiang, Y. Z. Wu and W. Xun, Built-in electric field and strain tunable valley-related multiple topological phase transitions in VSiX N4(X= C, Si, Ge, Sn, Pb) monolayers, *Phys. Rev. Mater.*, 2023, **7**, 064002.

36 N. Adir, S. Bar-Zvi and D. Harris, The amazing phycobilisome, *Biochim. Biophys. Acta - Bioenerg.*, 2020, **1861**, 148047.

37 A. N. Glazer, in *Photochemical and Photobiological Reviews*, Springer US, Boston, MA, 1976, pp. 71–115.
38 B. Stec, R. F. Troxler and M. M. Teeter, Crystal Structure of C-Phycocyanin from Cyanidium caldarium Provides a New Perspective on Phycobilisome Assembly, , DOI:10.1016/S0006-3495(99)77446-1.
39 S. A. Pizarro and K. Sauer, Spectroscopic Study of the Light-harvesting Protein C-Phycocyanin Associated with Colorless Linker Peptides†¶, *Photochem. Photobiol.*, 2001, **73**, 556.
40 J. M. Beechem and L. Brand, Time-resolved fluorescence of proteins, *Annu. Rev. Biochem.*, 1985, **VOL. 54**, 43–71.
41 D. M. Jameson and T. L. Hazlett, in *Biophysical and Biochemical Aspects of Fluorescence Spectroscopy*, Springer US, Boston, MA, 1991, pp. 105–133.
42 M. J. Limo, A. Sola-Rabada, E. Boix, V. Thota, Z. C. Westcott, V. Puddu and C. C. Perry, *Chem. Rev.*, 2018, 118, 11118–11193.
43 A. Vallee, V. Humblot and C.-M. Pradier, Peptide Interactions with Metal and Oxide Surfaces, , DOI:10.1021/ar100017n.
44 M. Geyer, R. Gutierrez, V. Mujica, J. F. R. Silva, A. Dianat and G. Cuniberti, The contribution of intermolecular spin interactions to the London dispersion forces between chiral molecules, *J. Chem. Phys.*, 2022, **156**, 234106.
45 Y. Kapon, Q. Zhu, S. Yochelis, R. Naaman, R. Gutierrez, G. Cuniberti, Y. Paltiel and V. Mujica, Probing chiral discrimination in biological systems using atomic force microscopy: The role of van der Waals and exchange interactions, *J. Chem. Phys.*, , DOI:10.1063/5.0171742/2928645.
46 N. Sukenik, F. Tassinari, S. Yochelis, O. Millo, L. T. Baczewski and Y. Paltiel, Correlation between Ferromagnetic Layer Easy Axis and the Tilt Angle of Self Assembled Chiral Molecules, *Molecules*, 2020, **25**, 6036.
47 I. Meirzada, ∇ N Sukenik, ∇ G Haim, ∇ S Yochelis, L. T. Baczewski, Y. Paltiel and N. Bar-Gill, Long-Time-Scale Magnetization Ordering Induced by an Adsorbed Chiral Monolayer on Ferromagnets, 2021, **15**, 2024.
48 I. Eisenberg, D. Harris, Y. Levi-Kalisman, S. Yochelis, A. Shemesh, G. Ben-Nissan, M. Sharon, U. Raviv, N. Adir, N. Keren and Y. Paltiel, Concentration-based self-assembly of phycocyanin, *Photosynth. Res.*, 2017, **134**, 39–49.
49 Y. Kolodny, H. Zer, M. Propper, S. Yochelis, Y. Paltiel and N. Keren, Marine cyanobacteria tune energy transfer efficiency in their light-harvesting antennae by modifying pigment coupling, *FEBS J.*, 2021, **288**, 980–994.
50 C. A. Royer, Understanding fluorescence decay in proteins., *Biophys. J.*, 1993, **65**, 9.
51 S. Kogan, *Electronic Noise and Fluctuations in Solids*, Cambridge University Press, illustrated, reprint., 1996.
52 N. Maroudas-Sklare, N. Goren, S. Yochelis, G. Jung, N. Keren and Y. Paltiel, Probing the design principles of photosynthetic systems through fluorescence noise measurement, *Sci. Reports 2024 141*, 2024, **14**, 1–8.
53 N. Peer, I. Dujovne, S. Yochelis and Y. Paltiel, Nanoscale Charge Separation Using Chiral Molecules, *ACS Photonics*, 2015, **2**, 1476–1481.
54 M. Gwizdala, T. P. J. Krüger, M. Wahadoszamen, J. M. Gruber and R. van Grondelle, Phycocyanin: One Complex, Two States, Two Functions, *J. Phys. Chem. Lett.*, 2018, **9**, 1365–1371.
55 J. Dai and X. Zhang, Chemical Regulation of Fluorescence Lifetime, *Cite This Chem. Biomed. Imaging*, 2023, **2023**, 796–816.
56 H. T. Fridman, J. Dehnel, S. Yochelis, E. Lifshitz and Y. Paltiel, Spin-Exciton Delocalization Enhancement in Multilayer Chiral Linker/Quantum Dot Structures, *J. Phys. Chem. Lett.*, 2019, **10**, 3858–3862.
57 S. Ghosh, K. Banerjee-Ghosh, D. Levy, I. Riven, R. Naaman and G. Haran, Substrates modulate charge-reorganization allosteric effects in protein−protein association, *J. Phys. Chem. Lett.*, 2021, **12**, 2805–2808.

# Data availability statement for manuscript titled:

*" Probing spin effects in Phycocyanin using Janus-like ferromagnetic microparticles"*

## By:

*Avi Schneider, Ilay David, Naama Goren, Hanna T. Fridman, Guy Lutzky, Shira Yochelis, Hagit Zer, Noam Adir, Nir Keren and Yossi Paltiel*

## The data supporting this article have been added to as part of the Supplementary Information